JOURNAL OF THE STRUCTURAL DIVISION

NONLINEAR CREEP BUCKLING OF REINFORCED CONCRETE COLUMNS

By Zdeněk P. Bažant,[1] F. ASCE and Tatsuya Tsubaki[2]

INTRODUCTION

The nonlinearity of the creep law profoundly influences the long-time buckling of reinforced concrete columns and can even cause a qualitative change in the behavior. For example, when the creep law is linear, as in viscoelasticity, the critical buckling time is infinite, whereas, for a nonlinear creep law, it can be finite, as has often been observed in tests of concrete columns. Nonlinear creep buckling of concrete columns has, therefore, been studied intensively and solutions which adequately model many aspects of the problem have been obtained (1,3,10,22,24,25,26,27,29,32,36). Especially comprehensive is the recent work by Fouré (14), in which the stress-dependent effective modulus is applied to approximate the creep effects, and practical formulas well supported by numerous experiments are obtained.

One aspect of the problem, however, has received relatively little attention. This is the behavior of columns which are for a long time subjected to a relatively low sustained load (dead load multiplied by its load factor) and then are suddenly overloaded (by the live load multiplied by its load factor). Among the few works on this practically important case is the excellent study by Drysdale and Huggins (13), in which the strength of prismatic, simply supported, reinforced concrete columns with square cross sections are examined under three kinds of biaxial eccentric loads: short-time loading to failure; sustained loading to failure; and sustained loading followed by short-time loading to failure. The experimental results are also compared with the results predicted by their mathematical model. A similar, very useful study was made by Kordina (21).

Until recently, however, a completely realistic analysis of the case of dead and live load was impossible because no model for the nonlinearity of creep at low (service) stress levels was available. In a preceding work (8), the experimental evidence was carefully analyzed; this resulted in a model characterized by two kinds of nonlinearity: (1) At high stress (stress exceeding about 65% of the strength), the creep is much higher than that predicted by a model based on the principle of superposition; whereas (2) at low stress (service stress levels), the creep due to the subsequent low increments is considerably less than that predicted by the principle of superposition. The latter nonlinearity, which was termed adaptation (8) and has been neglected in all previous studies of creep buckling of concrete columns, is important because, as the deflection of a column slowly grows and causes an increase of the bending moment due to the axial force, the creep due to subsequent increments of the bending moment is significantly less than previously considered. This tends to stiffen the response of the column and increase its long-time strength compared to the case where the sustained load is of high magnitude and causes stresses near the strength of concrete. This increase of strength is further augmented by the well-known fact that the sustained low compressive stress causes an increase of strength for subsequent sudden loads (9,15,18,31,33,34).

We choose it, therefore, as the objective of our work to analyze the effect of adaptation on the ultimate long-time strength of reinforced concrete columns and compare it to the long-time strength for a high sustained load. We will also compare the results with the present ACI Code and suggest its possible improvement.

Note.—Discussion open until April 1, 1981. To extend the closing date one month, a written request must be filed with the Manager of Technical and Professional Publications, ASCE. This paper is part of the copyrighted Journal of the Structural Division, Proceedings of the American Society of Civil Engineers, Vol. 106, No. ST11, November, 1980. Manuscript was submitted for review for possible publication on November 29, 1979.

[1]Prof. of Civ. Engrg., Northwestern Univ., Evanston, Ill.
[2]Grad. Research Asst., Northwestern Univ., Evanston, Ill.

REVIEW OF NONLINEAR CREEP LAW—ADAPTATION AND FLOW

Before analyzing the column, we need to give a brief review of the nonlinear creep law set up in Ref. 8. As proposed by McHenry (28), the uniaxial creep of concrete subjected to variable stress may be approximately determined by the principle of superposition

$$\epsilon(t) = \int_0^t J(t,t')\,d\sigma(t') \quad \ldots\ldots\ldots\ldots\ldots\ldots\ldots\ldots\ldots\ldots\ldots\ldots\ldots\ldots (1)$$

in which t = time = age of concrete; ϵ, σ = uniaxial strain and stress; and $J(t,t')$ = compliance (creep) function = strain at time t caused by a unit constant stress applied since time t'.

Although Eq. 1 accounts for the essential nature of creep in concrete, there exist significant nonlinear deviations, as found by Ross (30) and others. Two types of nonlinearity can be distinguished: (1) Adaptation: sustained compressive stress of working stress level makes the response to the subsequent load increments stiffer; and (2) Flow: high stress causes gradual weakening of response, i.e., a stress-dependent flow rate is to be added to the linear creep rate. Only the latter effect has been mathematically modeled in the previous works.

The nonlinearity is most properly described on the basis of creep rate, obtained by differentiating Eq. 1:

$$\dot{\epsilon}(t) = \frac{\dot{\sigma}(t)}{E(t)} + \int_0^t \dot{J}(t,t')\,d\sigma(t') \quad \ldots\ldots\ldots\ldots\ldots\ldots\ldots\ldots\ldots\ldots\ldots\ldots\ldots\ldots (2)$$

in which a superimposed dot stands for a derivative with respect to time t, and $E(t) = 1/J(t,t)$ = elastic modulus of concrete at time t.

Eq. 2 has been generalized (8) as follows:

$$\dot{\epsilon}(t) = \frac{\dot{\sigma}(t)}{E(t_e)} + \dot{\epsilon}_a(t) + \dot{\epsilon}_f(t) \quad \ldots\ldots (3)$$

$$\dot{\epsilon}_a(t) = g[\sigma(t)] \int_0^t \dot{J}(t,t'_e) \frac{d\sigma(t')}{1+a(t')}; \quad \dot{a}(t) = (a_1 + a_2 t^{-s}) \left[\frac{|I_1(t)|}{f'_c}\right]^r;$$

$$g[\sigma(t)] = a_3 + a_4 \{f[\sigma(t)]\}^n \quad \ldots\ldots (4)$$

$$\dot{\epsilon}_f(t) = \frac{\sigma(t) - \alpha(t)}{E_0} f[\sigma(t)]\,\dot{\phi}(t); \quad \dot{\phi}(t) = c_0 + c_1 t^{-q};$$

$$f[\sigma(t)] = \frac{J_2(t)}{c_2 + c_3\left[1 - \dfrac{\sqrt{3J_2(t)}}{I_1(t)}\right]};$$

$$\dot{\alpha}(t) = [\sigma(t) - \alpha(t)]\left[0.8 - \frac{\alpha(t)}{f'_c}\right]^3 (b_0 + b_1 t^{-p}) \quad \ldots\ldots (5)$$

$$dt_e = \beta_T \beta_h \beta_\sigma dt; \quad \beta_\sigma = 1 - a_0 I_1(t) \quad \ldots\ldots (6)$$

in which $I_1 = \sigma_{kk}$; and $J_2 = (1/2 s_{ij} s_{ij})^{1/2}$ = the second invariant of stress deviator. $\dot{\epsilon}_f(t)$, referred to as the flow rate, and $g[\sigma(t)]$ describe the high-stress nonlinearity, while $a(t)$, called the adaptation parameter, describes low-stress nonlinearity. Function $\dot{\phi}(t)$ decays with the age of concrete and models the stiffening of response with advancing hydration. In view of the fact that microcracking and plastic slip are caused mainly by shear distortion, the function $f[\sigma(t)]$ for high-stress nonlinearity is taken proportional to J_2. Function $\alpha(t)$ is used to express the range of stress under which high-stress nonlinearity occurs. The equivalent hydration period (or maturity), t_e, also models the low-stress nonlinearity, because coefficient β_σ gives acceleration of aging due to sustained compressive stress. Functions β_T and β_h introduce the effects of temperature, T, and relative humidity, h. They are chosen so that $\beta_T = 1$ for $T = 77°$ F (25° C) and $\beta_h = 1$ for $h = 100\%$.

Furthermore, f'_c = compressive cylinder strength of concrete at the age of 28 days. E_0 is the asymptotic modulus, which is obtained by extrapolation to infinitely fast loading (see Ref. 5).

Constants $a_0, \ldots, a_4, b_0, b_1, c_0, \ldots, c_3, n, p, q$, and r were all determined from experimental data. In the present study, the following values and relations are used (1 psi = 6.89 kPa):

$$a_0 = \frac{2}{f'_c}(\text{psi}); \quad a_1 = 0.1\left(\frac{\text{psi}}{f'_c}\right)^{1/2}; \quad a_2 = 2.4\left(\frac{\text{psi}}{f'_c}\right)^{1/2}; \quad a_3 = 0.98;$$

$$a_4 = 0.104; \quad b_0 = 10; \quad b_1 = 0; \quad c_0 = 0.5; \quad c_1 = 0; \quad c_2 = [0.3 f'_c(\text{psi})]^2;$$

$$c_3 = 0; \quad n = 1.5; \quad p = 0; \quad q = 0; \quad r = 0.5; \quad s = 0.5 \quad \ldots\ldots (7)$$

The compliance (creep) function $J(t,t')$ is assumed to follow the double power law $J(t,t') = [1 + \phi_1(t'^{-m} + \alpha)(t - t')^n]/E_0$, in which m, n, ϕ_1, α and E_0 are material parameters. Typical values for these parameters are found in Refs. 5 and 7. To model the effect of stress, temperature and humidity, the

double power law may be generalized as follows (4):

$$J(t,t') = \frac{1}{E_0} + \frac{\phi_1}{E_0}(t'^{-m}_e + \alpha)(t - t')^n \quad \ldots\ldots (8)$$

in which t'_e is obtained from Eq. 6. The parameters of this equation must be introduced so as to approximate the mean creep of the cross section with possible drying effect (7). This effect, which was studied by Wu and Huggins (37), will not be investigated here, however.

Algorithm of Numerical Structural Analysis

Structural analysis based on this creep law may be performed in small time steps. The flow of calculation is as follows.

1. Initialize variables at $t = 0$: $\sigma = 0$, $\epsilon = 0$, $\epsilon_a = 0$, $\epsilon_f = 0$, $a = 0$, and $\alpha = 0$.

2. For the jth time step, $\Delta t = t_j - t_{j-1}$, determine $\sigma(t_{j-1/2}) = \sigma(t_{j-1}) + \Delta\sigma/2$, $\beta_\sigma = 1 + a_0\sigma(t_{j-1/2})$, $\alpha(t_{j-1/2}) = \alpha(t_{j-1}) + \Delta\alpha/2$, $\Delta t_e = \beta_\sigma \Delta t$, and $t_{e_j} = t_{e_{j-1}} + \Delta t_e$ where $\Delta\sigma$ is taken as zero for the first iteration of the step. In subsequent iterations of the step, $\Delta\sigma$ may be taken as the value from the preceding iteration in order to achieve second-order accuracy.

3. As shown in Refs. 2 and 3, $\Delta\epsilon_a(t_j)$ may be determined by approximating the integral by the trapezoidal rule of integration:

$$E(t_{e_j}) = \frac{2}{J(t_{e_j}, t_{e_j}) + J(t_{e_j}, t_{e_{j-1}})} \quad \ldots\ldots (9)$$

$$\Delta J(t_j, t_{e_k}) = \frac{1}{2}[J(t_j, t_{e_k}) + J(t_j, t_{e_{k-1}}) - J(t_{j-1}, t_{e_k}) - J(t_{j-1}, t_{e_{k-1}})] \quad \ldots (10)$$

Next, calculate

$$\Delta a = (a_1 + a_2 t_{j-1}^{-s})\left[\frac{|\sigma(t_{j-1/2})|}{f'_c}\right]^r \Delta t;$$

$$f[\sigma(t_{j-1/2})] = \frac{\sigma^2(t_{j-1/2})}{3c_2}; \quad g[\sigma(t_{j-1/2})] = a_3 + a_4\{f[\sigma(t_{j-1/2})]\}^n \quad (11)$$

Then, $\Delta\epsilon_a$ may be obtained as

$$\Delta\epsilon_a = g[\sigma(t_{j-1/2})] \sum_{k=1}^{j-1} \Delta J(t_j, t'_{e_k}) \frac{\Delta\sigma(t_k)}{1 + a(t_k)} \quad \ldots\ldots (12)$$

4. Determine $\Delta\epsilon_f$:

$$\Delta\phi = c_0 \Delta t; \quad \Delta\alpha = \{\sigma(t_{j-1/2}) - \alpha(t_{j-1/2})\}\left[0.8 - \frac{\alpha(t_{j-1/2})}{f'_c}\right]^3 b_0 \Delta t \quad \ldots (13)$$

Then, $\Delta\epsilon_f$, defined by Eq. 5, is:

$$\Delta\epsilon_f = \frac{\sigma(t_{j-1/2}) - \alpha(t_{j-1/2})}{E_0} f[\sigma(t_{j-1/2})]\Delta\phi \quad \ldots\ldots\ldots\ldots\ldots\ldots (14)$$

5. Eq. 3 thus leads to an approximate quasi-elastic incremental stress-strain relation for the jth time step:

$$\Delta\sigma = E(t_j)\Delta\epsilon - \Delta\sigma_c; \quad \Delta\sigma_c = E(t_j)(\Delta\epsilon_a + \Delta\epsilon_f) \quad \ldots\ldots\ldots\ldots\ldots\ldots (15)$$

6. The changes of deformation and stresses in the structure during the jth time step may now be solved by an elastic analysis using Eq. 15, for example by the finite element method. This ultimately leads to increments of all stresses and strains, $\Delta\sigma$ and $\Delta\epsilon$, as well as $\Delta\epsilon_a$, $\Delta\epsilon_f$, Δa, $\Delta\alpha$, and to the values at the end of the jth step:

$$\sigma(t_j) = \sigma(t_{j-1}) + \Delta\sigma; \quad \epsilon(t_j) = \epsilon(t_{j-1}) + \Delta\epsilon; \quad \epsilon_a(t_j) = \epsilon_a(t_{j-1}) + \Delta\epsilon_a;$$

$$\epsilon_f(t_j) = \epsilon_f(t_{j-1}) + \Delta\epsilon_f; \quad a(t_j) = a(t_{j-1}) + \Delta a; \quad \alpha(t_j) = \alpha(t_{j-1}) + \Delta\alpha \qquad (16)$$

Then, one returns to step 2, iterates the process until an acceptable convergence is achieved, and then one goes to the next time step.

Sustained-Load Strength of Concrete

As mentioned before, a low sustained compressive load makes the response to the subsequent loading stiffer (adaptation or low-stress nonlinearity). Moreover, the compressive strength, f'_c, increases under a low sustained compressive load. Numerous experimental works document this fact.

Washa and Fluck (34) reported that, during 10.5 yr, the sustained loads (applied at age 28 days, equal to 25% of the initial strength) increased the strength of cylinders (6 in. (152 mm) in diameter, 12 in. (305 mm) high) that were kept in a drying condition (temperature 60° F–80° F (16° C–27° C), relative humidity 25%–60%) up to 5% compared with the specimens without sustained loads. Freudenthal and Roll (15) found f'_c in drying environment to increase by 2% to 30% in 1 yr, depending on concrete mix and specimen size. [In their tests, sustained loads of approximately 15%–65% of the 28-day compressive strength were applied at 28 days on cylinders of 3 in. and 4 in. (76 mm and 102 mm) in diameter and 10 in. (254 mm) high that were stored at 70° F (21° C) and 60% relative humidity.] Brettle (9) proposed empirical formulas for the change in strength and elastic modulus and reported a strength increase of up to 9% for a cylinder specimen [6 in. (152 mm) in diameter, 12 in. (305 mm) high] with 6,000 psi (41.3 MPa) nominal strength at 28 days. [In his tests, the test specimens with nominal strength 4,000 psi (27.6 MPa) and 8,000 psi (55.1 MPa) were loaded at 3 days to 7.5%–50% of the strength and then water-cured for 25 days before the final loading.] Stöckl (33) reported average increases from 3% to 18% and observed that the strength increased with increasing sustained load, increasing load period and decreasing concrete age at initial loading. [In his tests, sustained loads of 50%, 70%, and 90% of the strength at 28 days were applied at 3 days or 28 days on cylinders that were 5.9 in. (150 mm) in diameter and 11.8 in. (300 mm) high and were stored at 68° F (20° C) and 65% relative humidity. The load duration was 28 days or 196 days.] According to Hughes and Ash (18), the strength increases in drying environment from

4% to 13%. [In their tests, the specimens were prisms of 2 in. (51 mm) square by 4.75 in. (121 mm) long, loaded at ages 3 to 150 days for 25 days. The load was increased stepwise up to about 50% of the strength during the sustained load period.] Based on these test data, Hellesland and Green (17) proposed empirical formulas for the decrease of strength due to sustained loads that are constant up to failure. Their formulas, however, do not account for the increase of the short-time strength due to a previous low sustained load.

The creep law from Ref. 8 that we are using describes the nonlinear creep only up to about 90% or 95% of strength. To describe creep all the way to the strength value, the creep isochrones in σ-ϵ plots would have to reach a peak value with a horizontal tangent at the value of long-time strength, but the present creep law does not do that. Therefore, we must supplement it by a separate criterion for the long-time strength, and accept the fact that creep isochrones or other response curves terminate at the strength point with a finite slope rather than at a peak point with a horizontal tangent, as is seen in reality.

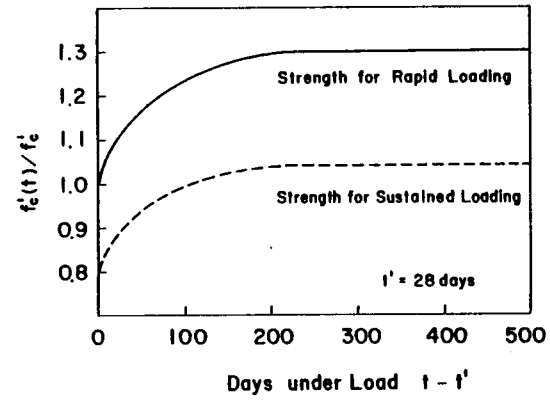

FIG. 1.—Influence of Sustained Loads on Strength of Concrete [Calculated from Present Nonlinear Creep Law with Same Creep Function as Shown in Fig. 3(e) for $P = 0.3Af'_c$]

We introduce a rather simple empirical relation for the sustained-load strength. ACI Building Code (11) gives the relation $E = 57{,}000(f'_c)^{1/2}$ where E = modulus of elasticity of concrete; and f'_c = strength (in pounds per square inch) of a cylindrical specimen tested at age 28 days. Approximately, this equation holds at various ages thus relating the growth of E and f'_c in time. From this equation we have:

$$f'_c(t) = f'_c\left[\frac{E(t)}{E_0}\right]^2 \quad \ldots\ldots\ldots\ldots\ldots\ldots\ldots\ldots\ldots\ldots (17)$$

With regard to load duration, it must be emphasized that f'_c is a strength for the loading rate or load duration that produces failure in about 5 min to 10 min, and Eq. 17 applies only to such load durations. At the point of failure, the stiffness of concrete is considered to drop to zero; we do not consider here any ductile response or strain-softening.

If the period of high stress is long, then, according to Rüsch (31), compressive strength is reduced to $0.8f'_c$ under sustained loads lasting about 7 days or more, where f'_c is the short-time strength measured at age 28 days. Therefore, if we want to study column failure due to buckling rather than due to pure material failure, we must limit our analysis to compressive stresses below $0.8f'_c$ in magnitude. For simplicity, we assume the increased short-time strength $f'_c(t)$ to be always reduced to $0.8f'_c(t)$ for long-time loading. However, we do not reduce the strength for short-time loading, regardless of the duration of the applied dead loads, i.e., whenever short-time loading is considered we apply Eq. 17.

The elastic modulus at age t, $E(t)$, appearing in Eq. 17, may be best obtained from the double power law as the effective modulus for load duration $t - t' = 0.001$ day, which gives

$$\frac{1}{E(t')} = \frac{1 + \alpha_1 t_e'^{-m}}{E_0}; \quad \alpha_1 = 0.001^n \phi_1 \quad \ldots\ldots\ldots\ldots\ldots\ldots\ldots\ldots \quad (18)$$

Note that t'_e is used instead of t' in order to take into account the effect of temperature, humidity, and stress on the change of elastic modulus.

Considering available test data [e.g., Washa and Fluck (34)], it appears that there is an upper limit of about 30% (beyond f'_c at 28 days) on the strength increase due to the combined effect of sustained loads and hydration. Therefore, we combine this fact with the relation, Eq. 17.

An example of the time-dependent compressive strength $f'_c(t)$ used in this study is shown in Fig. 1. The compliance (creep) function used for this example is the same as the one used in Fig. 3(*e*).

Numerical Solution

We consider only static deflections of simply supported prismatic columns that have a symmetric and symmetrically reinforced cross section and are sufficiently slender for the bending theory to apply (Fig. 2). Customary assumptions of the bending theory are made: (1) The displacements and strains are small; and (2) plane cross sections remain plane and normal to the centroidal axis. Further, we assume that the reinforcing bars have negligible bending stiffness, that no bond slip exists, and that the cross section area occupied by steel is negligible. We also assume that concrete cannot carry tensile stress and that the steel is elastic-perfectly plastic (Fig. 3).

The calculation may be divided into three stages: the first rapid loading; subsequent long-time deformation; and finally a further rapid loading to failure. No creep is considered for the first rapid loading stage, i.e., the load is assumed to be applied instantaneously.

Instantaneous Elastic Solution.—A conventional beam-column element for small deformation is used. The detail of the finite element formulation for a structural element shown in Fig. 2(*d*) is given in Appendix I. For the first instantaneous loading, the following stiffness equation is used:

$$[\mathbf{K} + P_0 \mathbf{K}_G]\,\dot{\mathbf{U}} = \dot{\mathbf{F}} + \dot{\mathbf{F}}_P \quad \ldots\ldots\ldots\ldots\ldots\ldots\ldots\ldots\ldots\ldots \quad (19)$$

in which $\mathbf{K}$ and $\mathbf{K}_G$ denote the conventional stiffness matrix and the geometric

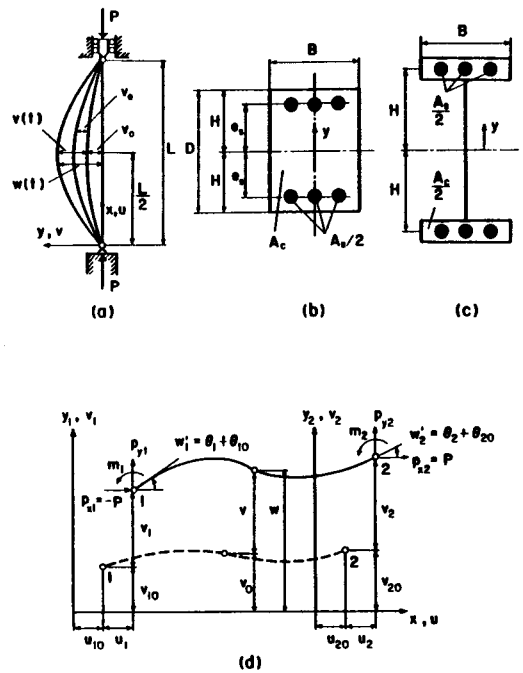

FIG. 2.—Reinforced Concrete Column with Initial Curvature: (*a*) Simply Supported Column; (*b*) Cross Section; (*c*) Idealized I-Section; (*d*) Notations for Beam-Column Element

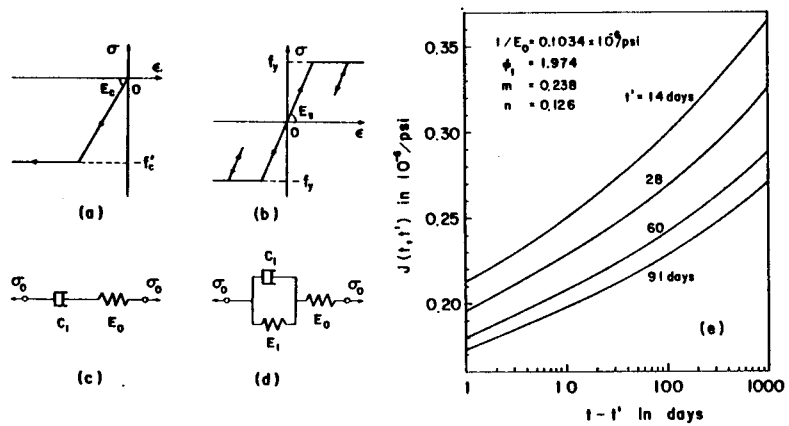

FIG. 3.—Constitutive Models: Simplified Stress-Strain Relations—(*a*) Concrete and (*b*) Steel; Linear Creep Models—(*c*) Maxwell Solid and (*d*) Standard Linear Solid; (*e*) Creep Function Used—Double Power Law (Ref. 5) [1 psi = 6.89 kPa]

stiffness matrix; P_0 is the initial axial load; U, F and F_P stand for a displacement vector, an external force vector, and an additional force vector reflecting the effect of the initial curvature, respectively; and superimposed dots indicate time derivatives. For more precise definitions, see Appendix I.

Time-Dependent Solution.—The time-dependent solution can be carried out as a sequence of elastic solutions with given inelastic strains. Since the elastic analysis of a column for arbitrary given inelastic strains is well-known (3), we do not need to further examine this approach.

The present problem has actually been solved by an alternate method in which one first determines, with the help of a variational principle, the matrix ordinary differential equations in time:

$$[\mathbf{K} + P_t \mathbf{K}_G]\,\dot{\mathbf{U}} = \dot{\mathbf{F}} + \dot{\mathbf{F}}_P + \dot{\mathbf{F}}_c \quad \ldots\ldots\ldots\ldots\ldots\ldots\ldots\ldots\ldots\ldots \quad (20)$$

This stiffness equation is solved by the standard step-by-step method for small time increments: K takes into account the change in the tangential moduli across the cross section; P_t is the axial force at time t; $\dot{\mathbf{F}}_P$ and $\dot{\mathbf{F}}_c$ stand for pseudo-force vectors reflecting the effect of the change in the axial force and that of the inelastic strain due to creep. Solving Eq. 20, the stress and strain in each element are calculated and the result is used to update the material constants. Then we proceed to the next iteration or time step. The solution generally converges well unless the column is failing. At that point, iterations of the step are omitted and either the Euler's method or the modified Euler's method is used together with sufficiently small time steps.

Illustrative Examples

The accuracy of the method of analysis described in the previous sections will first be examined by comparing the solutions for some simple problems with those obtained by other methods. A simply supported column with sinusoidal initial curvature is considered (Fig. 2). Since the present nonlinear creep law reduces to a linear one for $g = 1$, $a = 0$, $\alpha = \sigma$, and $t'_e = t'$, the present formulation can also be used for a linear creep model. We first consider simple idealized linear creep models (Fig. 3) such as

$$J(t,t') = \frac{1}{E_0} + \frac{1}{C_1}(t - t') \quad \text{(Maxwell Solid)} \quad \ldots\ldots\ldots\ldots\ldots \quad (21)$$

or

$$J(t,t') = \frac{1}{E_0} + \frac{1}{E_1}\left\{1 - \exp\left[-\frac{E_1}{C_1}(t - t')\right]\right\} \quad \text{(Standard Linear Solid)} \quad (22)$$

in which we use $E_0 = 5.0 \times 10^6$ psi (3.45×10^4 MPa), $E_1 = 5.0 \times 10^5$ psi (3.45×10^3 MPa), and $C_1 = 2.0 \times 10^8$ psi·day (1.38×10^6 MPa·day). The initial deflection at midspan is chosen as $v_0 = 0.025$ in. (0.64 mm) and the column load as $P = 2.0 \times 10^4$ psi (1.38×10^2 MPa) $= 0.3P_E$, where P_E is the Euler buckling load. The column is considered unreinforced and its dimensions are: the cross-sectional area $A = 25$ sq in. (1.61×10^4 mm^2); the half-depth of the cross section $H = 2.887$ in. (73.33 mm); the width of the cross section $B = 4.330$ in. (110.0 mm); and the column length $L = 200$ in. (5.08 m). To

avoid the numerical error due to integration over the cross section (see Appendix I), instead of a square cross section we consider in the examples an idealized two-layer section as shown in Fig. 2(*c*). The calculated variation of the deflection at midspan is shown in Fig. 4(*a*). Close agreement with the analytical solution (19,23) is obtained even when only four beam elements are used. No appreciable difference is observed when eight elements are used.

Kempner (20) solved a problem of a column with the nonlinear creep law:

$$\dot{\epsilon} = \frac{\dot{\sigma}}{E_0} + \frac{\sigma^m}{C_1} \quad \ldots\ldots\ldots\ldots\ldots\ldots\ldots\ldots\ldots\ldots\ldots\ldots\ldots\ldots \quad (23)$$

and he showed that, unlike a linear creep law, the nonlinear one yields an

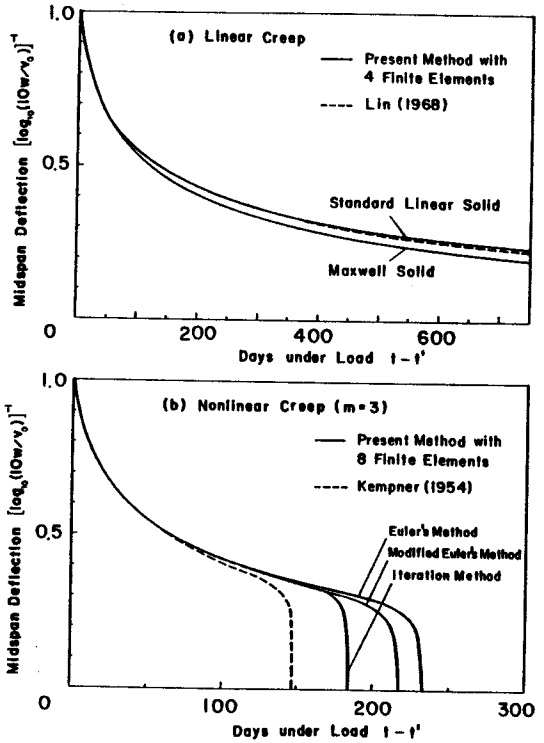

FIG. 4.—Midspan Deflection of Column with Simple Creep Law: (*a*) Linear Creep; (*b*) Nonlinear Creep

infinitely large deflection in a finite period of time. For $E_0 = 5.0 \times 10^6$ psi (3.45×10^4 MPa), $C_1 = 2.0 \times 10^{14}$ psi·day (1.38×10^{12} MPa·day), $m = 3$, the same column was solved. Comparison between Kempner's analytical solution obtained by the collocation method and the present finite element solution is shown in Fig. 4(*b*). The difference between the two methods becomes substantial when the deflection becomes large. This discrepancy seems to come from the approximations in the collocation method and the present finite element method.

The influence of the time integration method appears to be significant. Shown in Fig. 4(*b*) is the difference among the solutions by the iteration method, Euler's method, and the modified Euler's method in which one half of the previous increment is added to each total value at the end of the previous step in order to evaluate the nonlinear creep strain rate. Again, the difference due to the number of elements is not appreciable. With the aforementioned simple nonlinear creep law which is valid both for compression and tension if m is an odd integer, the variation of deflection could be followed even when the deflection becomes 10^4 times as large as the initial elastic deflection. Therefore, it was easy to obtain the critical time graphically, as shown in Fig. 4(*b*). The large deflections occurring near the critical time are of course not actually possible since the material has a finite strength and deforms together with elastic-plastic steel bars. The criterion to get the critical time for these cases will be indicated in the corresponding text.

Having shown that our solution method is sufficiently accurate, a reinforced concrete column with sinusoidal initial curvature has been solved to examine the influence of the nonlinearity due to adaptation and flow. For simplicity, first an idealized I-cross section is used [Fig. 2(*c*)]. The dimensions of the column are: $A = 25$ sq in. (1.61×10^4 mm^2); $H = e = 2.887$ in. (73.33 mm); $B = 4.330$ in. (110.0 mm); $L = 100$ in. (2.54 m). This area and the corresponding moment of inertia are equivalent to those for a square cross section with a side of 5 in. (127 mm). The creep function used in the calculation is plotted in Fig. 3(*e*). The parameters used in this double power law are: $E_0 = 1/(0.1034 \times 10^{-6})$ psi ($1/(0.1501 \times 10^{-4})$ MPa); $\phi_1 = 1.974$; $m = 0.238$; $n = 0.126$ (from Ref. 5 for Ross's creep data). The other parameters are fixed as follows: the ratio of initial curvature at midspan to the depth of the cross section $v_0/D = 0.01$; slenderness ratio $L/D = 20$; reinforcement ratio $\rho = 0.01$ and 0.02. A simplified instantaneous stress-strain relation was assumed for both concrete and steel reinforcement as shown in Fig. 3(*a,b*), where $f'_c = 6{,}700$ psi (46.2 MPa), f_y =i40,000 psi (276 MPa) and $E_s = 3.0 \times 10^7$ psi (2.07×10^5 MPa). The load is assumed to be applied at age 28 days.

First the case of constant axial load has been examined. The calculated deflection-time relation is shown in Fig. 5 for various levels of the load. The occurrence of excessive deflection, at least 10-times larger than the initial elastic deflection, and an abrupt change in the deflection rate have been considered as indications of failure of the column. We see from the calculations that the larger the load, the shorter is the critical time. It is also observed that, for large loads, the column fails in a rather brittle manner, i.e., by an abrupt increase of the deflection rate. This phenomenon is, however, spurious since it is due to the assumption that a failure (strength) does not correspond to a point of horizontal tangent on the stress-strain curve. A low stress such as $\sigma_0 = 0.3f'_c$ [Fig. 5(*a*)] has not produced large deflection even after 10,000 days. It is also seen that the column with more reinforcement is more creep resistant. The failure envelope for constant loads is shown in Fig. 6.

Next, the case in which the load is suddenly increased up to failure after a long period of constant load has been examined (see examples of loading paths marked by arrows in Fig. 6). For convenience of calculation, a finite constant stress rate, $0.01f'_c/0.0002$ day, has been chosen for this rapid loading. The column strength for this loading has been examined for various values

and durations of the sustained constant load. The results are exhibited in Fig. 6. The short-time strength of the column increases because of the increase

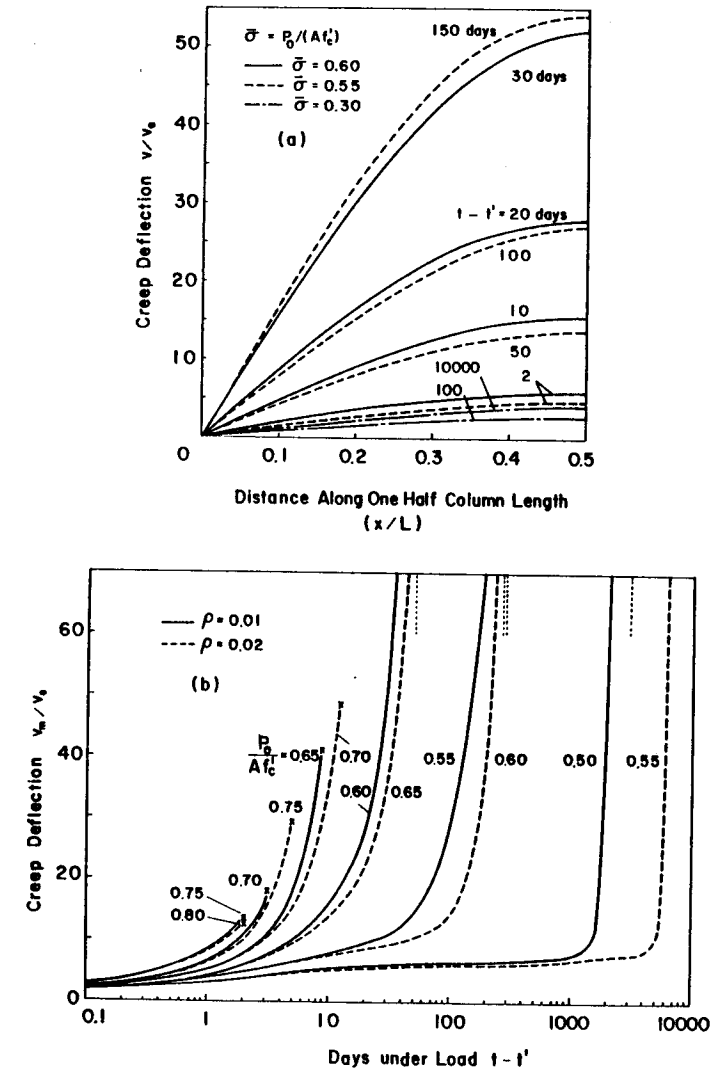

FIG. 5.—Creep Deflection, v, of Column with Nonlinear Creep Law (Ref. 8) Using Creep Function Shown in Fig. 3(*e*): (*a*) Deflection Profiles at Various Times; (*b*) Deflection at Midspan, v_m [v_e = elastic deflection at midspan, $v_0/D = 0.01$, $L/D = 20$, $f'_c = 6{,}700$ psi (46.2 MPa), $\rho = 0.01$, P_0 = constant sustained load, $A = 25$ sq in. (1.61×10^4 mm^2)]

in concrete strength, as described in the previous sections, while it decreases as the creep deformation due to the sustained load grows. Thus, the short-time failure envelope eventually comes down to the constant load failure envelope

upon reaching the critical time. Using these results, isochronous response curves for the column deflections are drawn in Fig. 7(*a*). Calculations show that indeed the response of a column becomes stiffer after it has been subjected to a low stress for a longer period. For the same duration of the constant sustained

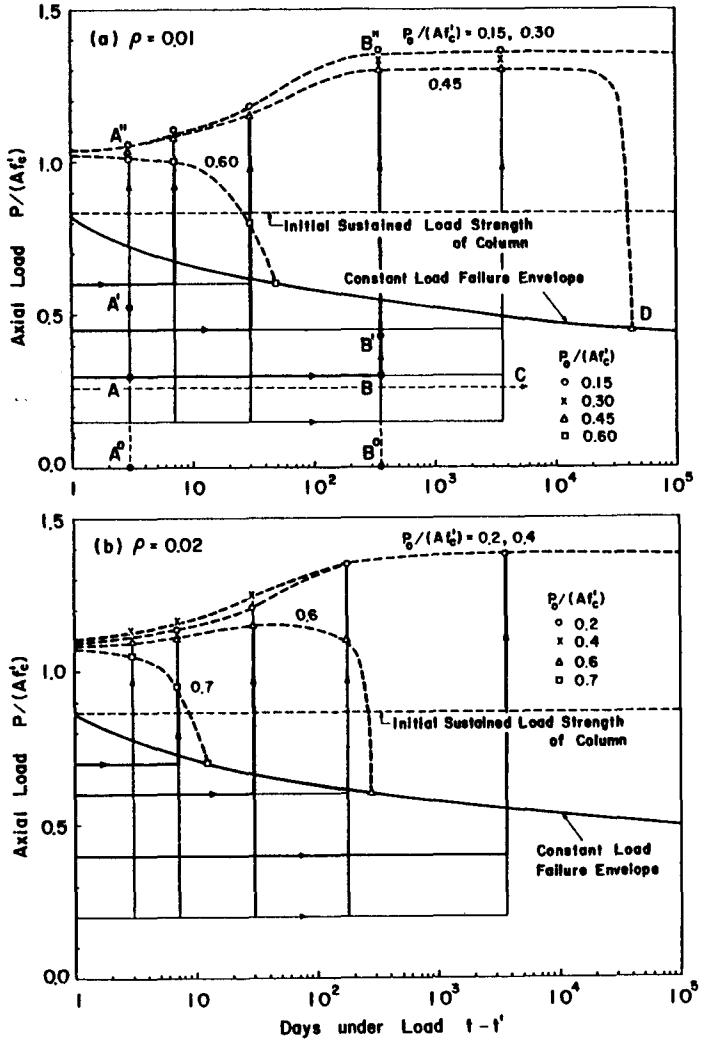

FIG. 6.—Calculated Failure Envelopes for Constant Sustained Loading and for Rapid Loading: (*a*) $\rho = 0.01$, $\sigma_E/f'_c = 2.252$; (*b*) $\rho = 0.02$, $\sigma_E/f'_c = 2.344$ (σ_E = Euler buckling stress; other data are given in Fig. 5 caption)

load, a lower (but not very low) sustained stress causes a stiffer subsequent response. This result is due to the adaptation nonlinearity at low stresses and the flow nonlinearity at high stresses.

The effect of these nonlinearities on the strain increments, $\Delta\epsilon_a$ and $\Delta\epsilon_f$ (defined by Eqs. 12 and 14) is shown in Fig. 7(*b*). $\Delta\epsilon_a$ and $\Delta\epsilon_f$ are the values for the second load increment of the stress rate, $0.05f'_c/0.001$ day, in the rapid loading,

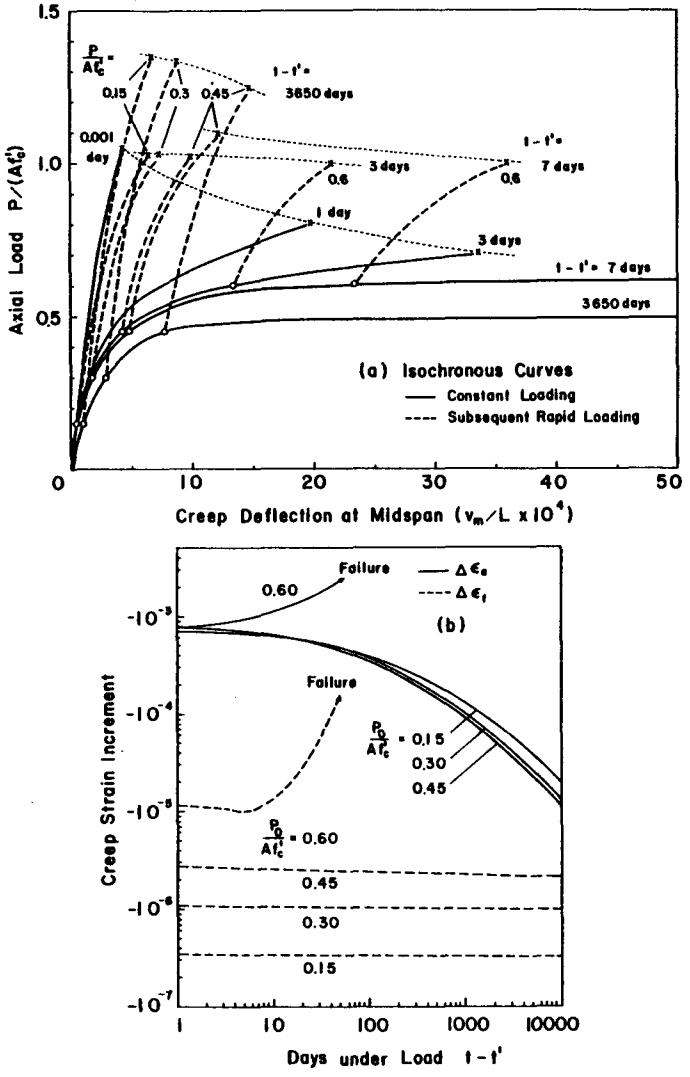

FIG. 7.—High Stress Nonlinearity and Low Stress Nonlinearity: (*a*) Isochronous Curves of Initial Axial Load versus Creep Deflection at Midspan; (*b*) Creep Response in Subsequent Rapid Loading [L = 100 in. (2.54 m), $\rho = 0.01$; other data are given in Fig. 5 caption]

measured at the compression face at the midspan. For a relatively high stress, $\sigma_0 = 0.6f'_c$, both $\Delta\epsilon_a$ and $\Delta\epsilon_f$ increase as the critical time approaches. On

the other hand, $\Delta\epsilon_a$ for a lower stress, such as $\sigma_0 \leq 0.45f'_c$, decreases as time increases, which makes the response stiffer. We may also note that the compressive stress in concrete tends to decrease all over the cross section if the transverse deflection is not very large; this well-known effect is, of course, caused by gradual transfer of load from the creeping concrete onto the reinforcement which does not creep. Since $\Delta\epsilon_f$ is proportional to the stress, $\Delta\epsilon_f$ slightly decreases for a lower column load.

Comparison with Test Data

A comparison with the test data by Drysdale and Huggins (13) has also been made. The creep law used in their work has been approximated, for convenience

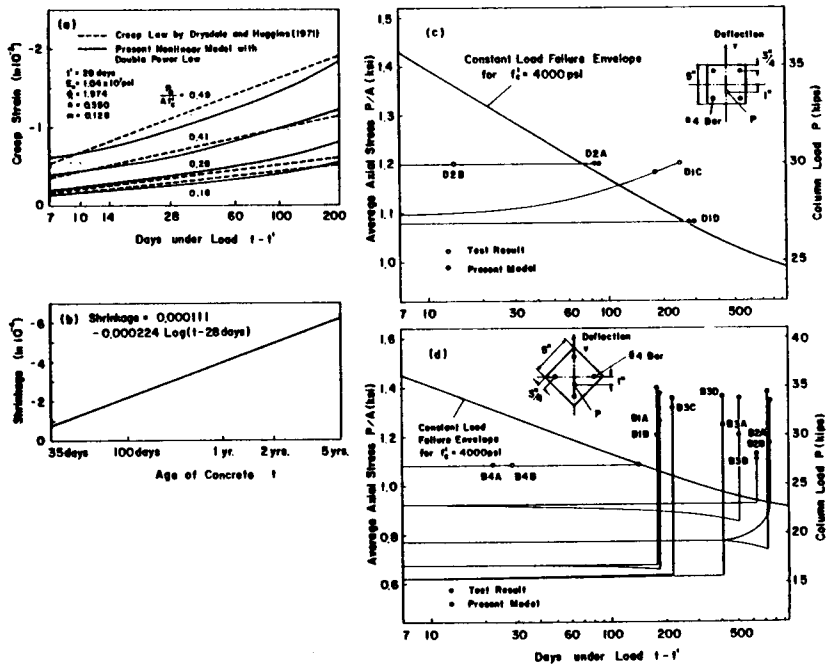

FIG. 8.—Comparison with Test Data by Drysdale and Huggins (13): (*a*) Creep Strain; (*b*) Shrinkage; (*c, d*) Sustained Load Strength of Column [L = 156 in. (3.96 m), ρ = 0.03, A = 25 sq in. (1.61 × 10⁴ mm²), L/D = 31, E_s = 30.0 × 10⁶ psi (2.07 × 10⁵ MPa) f_y = 56,080 psi (386 MPa), t' = 28 days] (1 ksi = 6.89 MPa, 1 kip = 453 kg)

of calculations, by the double power law with parameter values for which the difference is sufficiently small (see Fig. 8). Four elements were used for the half-length of column and each cross section was divided into five layers. For uniaxial buckling (in the plane of symmetry) due to an eccentrically applied load, a reasonable agreement has been obtained, as shown in Fig. 8.

A similar comparison with test data by Kordina (21) is shown in Fig. 9.

The double power law and the square-root hyperbolic law were used to approximate the test data on creep and shrinkage of column VII, respectively (see Fig. 9). The relations of creep and shrinkage for column VII have been used for all the columns. The column was discretized in the same way as for the previous comparison to analyze the column strength for the final short-time loading. In all the cases, the columns were unloaded after the sustained load for a certain period before applying the final short-time load as described in the test data. The results are in satisfactory agreement with the reported measurements.

By contrast, when using linear superposition with the same creep function, calculations for a high stress close to $0.8f'_c$ have not indicated failure even

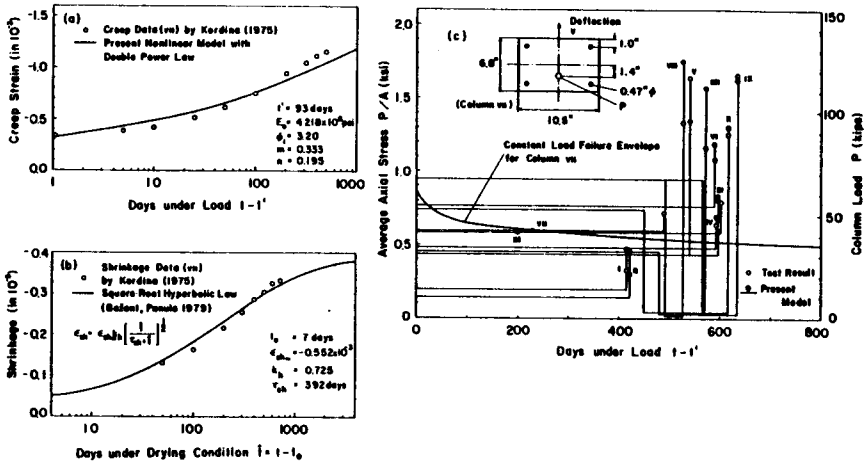

FIG. 9.—Comparison with Test Data by Kordina (21): (*a*) Creep Strain; (*b*) Shrinkage; (*c*) Sustained Load Strength of Column [L = 202.4 in. (5.14 m), A = 71.3 sq in. (4.60 × 10⁴ mm²), L/D = 30] (1 ksi = 6.89 MPa, 1 kip = 453 kg)

after 10,000 days of loading, despite the use of a finite strength limit for concrete and steel. This is probably due to the stabilizing effect of reinforcement.

Comparison with ACI Code and New Design Formula

It is interesting to compare the results in Fig. 6 with ACI Code (11). We consider the idealized I-section [Fig. 2(*c*)] used for Fig. 6. From ACI Code equation 10.9, we get $EI(1 + \beta_d) = 8.89 \times 10^7$ lb sq in. (2.60×10^{10} kg mm²) for $\rho = 0.01$, in which EI = bending stiffness. Assuming sinusoidal deflection with maximum ordinate v_0 we have from ACI Code $\beta_d = 1.4Dv_0/[(1.4D + 1.7L)v_0] = 1.4D/(1.4D + 1.7L)$ in which D is the axial dead load (sustained load) and L is the axial live load (rapidly applied load that leads to failure). In Fig. 6(*a*) we assume that there is a sustained load up to point B (or A) followed by a rapid load increase represented by a vertical line from point B (or A). For point B, the sustained load is exemplified by segment B^0B and the live load by segment BB''. ACI Code (11) does not distinguish between

various durations of the dead load. The load duration for point A in Fig. 6(*a*) is so short (3 days) and our calculated failure load (point A″) is so close to the instantaneous end of the failure envelope that one may consider the total load represented by segment A^0A'' as the live load; so, $\beta_d = 0$. According to ACI Code (11) Eq. 10.8, the ultimate load for a column in which the initial bending moments are very small is less than but rather close to the value $P'_u = \pi^2 EI/(kl)^2$, in which $l = 100$ in. (2.54 m) and $k = 1.0$. For the short-time loading ($\beta_d = 0$) we than get $P'_u/Af'_c = 0.524$, which is plotted as point A′ in Fig. 6(*a*). Point B in Fig. 6(*a*) represents a sustained load of considerable duration (1 yr) and should no doubt be considered as the dead load, represented by segment B^0B. On the vertical line through point B we then read from Fig. 6(*a*) $BB''/B^0B = 1.03/0.30$. Noting that the load factors for the dead and live loads are 1.4 and 1.7, we have $1.7L/1.4D = 1.03/0.30$ from which $L/D = 2.83$. This yields $\beta_d = 0.3/(1.03 + 0.30) = 0.226$, from which we get for the ultimate load the result $P'_u/Af'_c = 0.427$. This is plotted as point B′ in Fig. 6(*a*). In case that all load is a sustained load (dead load), we have $\beta_d = 1.0$ and we get $P'_u/Af'_c = 0.262$, which is shown as line C in Fig. 6(*a*).

TABLE 1.—Comparison with ACI Code

Loading (1)	β_d (2)	P^*/Af'_c (3)	P'_u/Af'_c (4)	P/Af'_c (5)	P^*/P'_u (6)	P^*/P (7)	P'_u/P (8)
Live load only	0	1.05	0.524	0.216	2.00	4.86	2.43
Live plus dead loads	0.266	1.33	0.427	0.184	3.11	7.23	2.32
Dead load only	1	0.445	0.262	0.131	1.70	3.40	2.00

Note: β_d = ratio of maximum factored dead load moment to maximum factored total (dead plus live) load moment; P^* = failure load calculated by the present method; P'_u = ultimate column capacity by ACI Code; P = corresponding total (dead plus live) design load; P^*/P and P'_u/P = safety factors from present results and by ACI Code.

Now we may determine the ratios of our calculated failure loads P^* to the failure loads P'_u according to the ACI Code (Table 1). For the short-time load (live load), this ratio is $P^*/P'_u = A^0A''/A^0A' = 1.05/0.524 = 2.00$. For the dead plus live load this ratio is $P^*/P'_u = B^0B''/B^0B' = 1.33/0.427 = 3.11$, and for the sustained load (dead load) alone, this ratio equals the ratio of the ordinates of point D and line C in Fig. 6(*a*), which gives $P/P'_u = 0.445/0.262 = 1.7$. We see that ACI Code gives safe and rather conservative estimates for the failure load. We also see that the values of P^*/P'_u, representing the extra safety margin, are not too different for the live load alone and the dead load alone, but are much higher for the combination of dead and live load (see Table 1).

Although the safety factor P^*/P, i.e., the ratio of the failure load P^* to the total design load $P = D + L$, is not used in ACI Code, it is also interesting to compare its values. Noting that for tied columns the capacity reduction factor is 0.7, the safety factor for live load alone is according to ACI Code $1.7/0.7 = 2.43$; for dead load alone it is $1.4/0.7 = 2.00$; and when $L/D = 2.83$, it is $(1.7 \times 2.83 + 1.4)/[(2.83 + 1)\,0.7] = 2.32$. The corresponding design loads

$D + L = P$ are given by $P/Af'_c = 0.524/2.43 = 0.216$ for the live load alone, $0.262/2.00 = 0.131$ for the dead load alone, and $0.427/2.32 = 0.184$ for $L/D = 2.83$; see Table 1. From our results, the safety factors P^*/P are $1.05/0.216 = 4.86$ for the live load alone, $0.445/0.131 = 3.40$ for the dead load alone, and $1.33/0.184 = 7.23$ for $L/D = 2.83$. Again we see that for the combined live plus dead load the safety factor is much larger than for either live load or dead load alone (Table 1).

The ratio of failure load under live load (short-time load) alone is according to Eq. 10.9 of ACI Code (11) given by the factor $(1 + \beta_d)$, whose plot against β_d is shown in Fig. 10. Using points B and B″ as an example, we have already shown how to calculate the ratio of factored dead and live loads for any failure point in Fig. 6. This calculation has been performed for many failure points from Fig. 6 and the results are plotted as the points in Fig. 10(*a*).

Although done neither by Drysdale and Huggins (13) nor Kordina (21), we may cast the results of their column tests in the same form as Fig. 10(*a*).

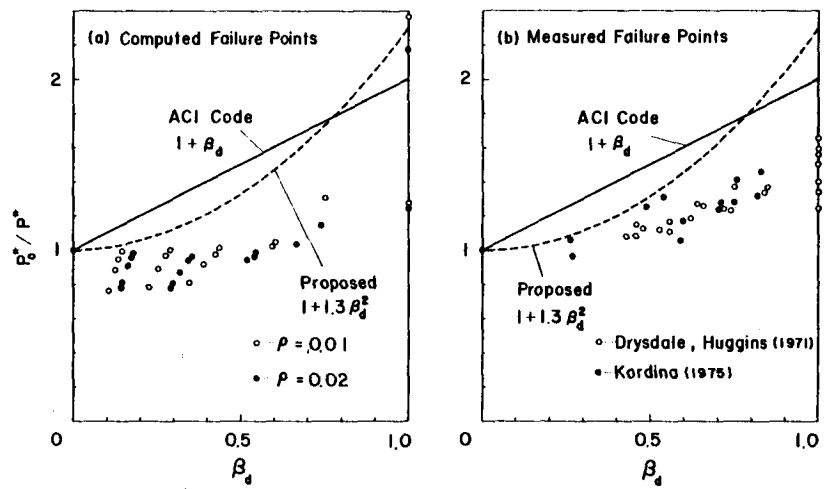

FIG. 10.—Ratio of Column Failure Load under Combined Dead and Live Load, P^*, to that under Live Load Alone, P_0^*: (*a*) Calculated Points; (*b*) Results of Tests from Refs. 13 and 21

This is done in Fig. 10(*b*), in which the data points represent all the 44 column failure tests reported by those experimentalists (only 36 points can be distinguished though, since some coincide). It should be noted that some of Kordina's columns were unloaded for periods from 0.4 day to 167 days after the sustained load and before the final rapid loading to failure; this has been ignored in plotting the points in Fig. 10(*b*) but did not seem to cause disruption of the overall trend. Neither did the fact that in a few of Drysdale and Huggins' tests the sustained load was slightly increasing or decreasing (by not more than 12%); those cases were evaluated as if the sustained load were constant and equal to the average of its initial and final values.

From Fig. 10(*a*) we see that the ACI factor $(1 + \beta_d)$ does not agree very

well with our results. For $0.2 \leq \beta_d \leq 0.75$ it is unnecessary conservative, and for $\beta_d > 0.9$ the safety margin is according to Fig. 10(*a*) lower than that for the short-time load. The safety and economy are in proper balance when the safety margins (relative to factored loads) are uniform. We propose, therefore, that the current factor $(1 + \beta_d)$ in ACI Code be replaced by the formula

$$\frac{P_0^*}{P^*} = 1 + 1.3\beta_d^2 \quad \ldots\ldots\ldots\ldots\ldots\ldots\ldots\ldots\ldots\ldots\ldots\ldots\ldots\ldots\ldots\ldots\ldots\ldots \quad (24)$$

This is plotted as the dashed curves in Fig. 10(*a,b*) and represents a common envelope to all points, experimental as well as calculated.

It may be noted that a straight line would envelop the available experimental points in Fig. 10(*b*) even better than the proposed curve. However, we must realize that the direct experimental evidence in Fig. 10(*b*) is (and will remain) of limited time range; none of the available column tests (13,21) exceed 2 yr of sustained load duration, while the uppermost calculated failure points in Fig. 10(*a*) correspond to a 30-yr load duration (the high location of these points is due chiefly to the large creep deflection). It is because of these points that the curve should be parabolic rather than linear in β_d.

It must be also emphasized that the calculated points in Fig. 10(*a*) are not just theoretical results but indirect logical consequences of diverse experimental evidence used to calibrate our theory. It would be also possible to set up an expression which would distinguish between the points on the top and bottom sides of the band in Fig. 10(*a,b*). However, this would require introduction of further parameters, such as the duration of sustained load, which would be hard to estimate for the designers.

Summary and Conclusions

The long-time strength of reinforced concrete columns is investigated by using the previously developed new model for nonlinear creep of concrete (8) which accounts not only for the increase of creep at high compressive stress (flow) but also for the decrease of creep for subsequent load increments (adaptation) caused by low sustained compressive stress. Also considered is the decline of long-time strength with the duration of a high constant sustained load and the increase of strength for rapid loading that follows a low sustained compressive stress. The deflection histories are solved numerically by the finite element method with small time increments. The effect of the nonlinearities, especially the adaptation, is examined by solving typical examples for load histories of three types: (I) Constant sustained load until failure; (II) high or (III) low constant sustained load followed by a sudden load increase until failure. Calculations confirm that the flow nonlinearity makes the column fail in a finite time (critical time). The basic conclusions are:

1. There is a great difference in strength between loading cases I, II and III, and the effect of dead-to-live load ratio is substantial.
2. Case III leads to a much higher load at failure than do cases I and II. The failure load can be up to about 35% higher than the failure load for instantaneous loading up to failure, and up to 100% higher than the constant sustained load leading to failure within the same time period.
3. This could be taken into account in setting the load factors for columns subjected to dead and live loads of various ratios.
4. The increase of failure load for a low constant sustained load is due to the recently discussed phenomenon of adaptation nonlinearity in creep.
5. The adaptation causes the response to subsequent sudden overload to become stiffer and the strength higher as the duration of the low constant load increases.
6. The results of the present method of analysis are in satisfactory agreement with the available experimental results.
7. The present ACI Code (11) does not give uniform safety margins for various ratios of dead and live loads. When the factored dead load represents 0.2–0.75 of the total factored load, the safety margin of ACI Code is much higher than that for the live load alone, and when this ratio exceeds 0.9 it is lower.
8. An improved expression to take into account the ratio of dead and live loads is proposed.

Acknowledgment

Support of the National Science Foundation under Grant ENG75-14848-A01 to Northwestern University is gratefully acknowledged. The first writer also obtained partial support under Guggenheim Fellowship awarded to him for 1978–79.

Appendix I.—Derivation of Stiffness Equation

Consider a beam element which is in equilibrium under the external forces, as shown in Fig. 2(*d*). Assuming that deformation is small, the strain-displacement relation of a beam with small deflection, v_0, due to the initial curvature is determined as follows (35):

$$\epsilon = u' + v_0' v' + \frac{1}{2}(v')^2 - yv'' \quad \ldots\ldots\ldots\ldots\ldots\ldots\ldots\ldots\ldots\ldots\ldots\ldots \quad (25)$$

in which u and v stand for the axial displacement and the transverse displacement. A superimposed prime means differentiation with respect to x. The third nonlinear term represents a strain component associated with the coupling of flexural and axial action. Considering a constitutive relation, $\sigma = E\epsilon - \sigma_c$, in which E is a function of σ and σ_c is the pseudo-stress, substitution of Eq. 25 yields

$$\sigma = E\left[u' + v_0' v' + \frac{1}{2}(v')^2 - yv''\right] - \sigma_c \quad \ldots\ldots\ldots\ldots\ldots\ldots\ldots\ldots \quad (26)$$

For the beam element shown in Fig. 2(*d*), the virtual work equation becomes as follows:

$$\int_0^L \int_A \sigma \delta\epsilon \, dA \, dx = m_2 \delta v_2' + m_1 \delta v_1' + p_{x_2} \delta u_2 + p_{x_1} \delta u_1 + p_{y_2} \delta v_2 + p_{y_1} \delta v_1 \quad \ldots\ldots\ldots\ldots\ldots\ldots\ldots\ldots \quad (27)$$

in which A and L denote the cross-sectional area and the element length; and

m, p_x and p_y respectively stand for the applied moment, the axial force, and the lateral force at nodes 1 and 2. Substituting Eqs. 25 and 26 into the left-hand side of Eq. 27, the following is obtained:

$$\int_0^L \int_A \sigma \delta \epsilon \, dA \, dx = \int_0^L \left[\int_A (\delta u' E u' + \delta v'' E y^2 v'') \, dA + \delta v' P v' \right] dx$$
$$+ \int_0^L \delta v' P v_0' \, dx - \int_0^L \int_A (\delta u' \sigma_c - \delta v'' \sigma_c y) \, dA \, dx$$
$$- \int_0^L \int_A (\delta u' E y v'' + \delta v'' E y u') \, dA \, dx \quad \ldots\ldots\ldots\ldots\ldots\ldots \quad (28)$$

in which higher-order terms have been neglected and $P = \int_A \sigma \, dA$. The following linear and cubic shape functions are used for displacements u and v:

$$u = \mathbf{L}(x)\mathbf{U}; \quad \mathbf{L}(x) = \{1 - \xi, 0, 0, \xi, 0, 0\};$$
$$v = \mathbf{H}(x)\mathbf{U}; \quad \mathbf{H}(x) = \{0, 1 - 3\xi^2 + 2\xi^3, L(\xi - 2\xi^2 + \xi^3), 0, 3\xi^2$$
$$- 2\xi^3, L(-\xi^2 + \xi^3)\}; \quad \text{where} \quad \mathbf{U} = \{u_1, v_1, \theta_1, u_2, v_2, \theta_2\}^T \quad \ldots\ldots\ldots \quad (29)$$

and $\theta = v'$; $\xi = X/L$; and T represents a transpose. Substitution of Eq. 29 into Eq. 27 yields

$$[\mathbf{K} + P\mathbf{K}_G]\mathbf{U} = \mathbf{F} + \mathbf{F}_P + \mathbf{F}_c \quad \ldots\ldots\ldots\ldots\ldots\ldots\ldots\ldots \quad (30)$$

in which

$$\mathbf{K} = \mathbf{K}_0 + \mathbf{K}^*; \quad \mathbf{K}_0 = \int_0^L [\alpha \mathbf{L}'^T \mathbf{L}' + \beta \mathbf{H}''^T \mathbf{H}''] \, dx;$$
$$\mathbf{K}^* = -\int_0^L \gamma \, [\mathbf{L}'^T \mathbf{H}'' + \mathbf{H}''^T \mathbf{L}'] \, dx; \quad \mathbf{K}_G = \int_0^L \mathbf{H}'^T \mathbf{H}' \, dx;$$
$$\mathbf{F} = \{p_{x_1}, p_{y_1}, m_1, p_{x_2}, p_{y_2}, m_2\}^T; \quad \mathbf{F}_P = -P\mathbf{K}_G\mathbf{U}_0;$$
$$\mathbf{U}_0 = \{u_{0_1}, v_{0_1}, \theta_{0_1}, u_{0_2}, v_{0_2}, \theta_{0_2}\}^T; \quad \mathbf{F}_c = \int_0^L [p_c \mathbf{L}' - m_c \mathbf{H}''] \, dx$$
$$\alpha = \int_A E \, dA; \quad \beta = \int_A E y^2 \, dA; \quad \gamma = \int_A E y \, dA;$$
$$p_c = \int_A \sigma_c \, dA; \quad m_c = \int_A \sigma_c y \, dA \quad \ldots\ldots\ldots\ldots\ldots\ldots\ldots\ldots \quad (31)$$

α, β, γ, p_c and m_c are evaluated at the middle of the element and are assumed to be constant in each element. The detail of the form of the matrices may be found in Refs. 12, 16, and 38. For an elastic solution, $\mathbf{K}^* = \mathbf{0}$, and $\mathbf{F}_c = \mathbf{0}$. The incrementally linear form of Eq. 30 is thus obtained as

$$[\mathbf{K} + P\mathbf{K}_G]\dot{\mathbf{U}} = \dot{\mathbf{F}} + \dot{\mathbf{F}}_P + \dot{\mathbf{F}}_c \quad \ldots\ldots\ldots\ldots\ldots\ldots\ldots\ldots \quad (32)$$

in which $\dot{\mathbf{F}}_P = -P\mathbf{K}_G(\dot{\mathbf{U}} + \dot{\mathbf{U}}_0)$, and the other quantities with a superimposed dot are obtained by differentiating the relations in Eq. 31 with respect to time (see also Ref. 6).

Appendix II.—References

1. Bažant, Z. P., "Creep Stability and Buckling Strength of Concrete Columns," *Magazine of Concrete Research*, Vol. 20, 1968, pp. 85–94.
2. Bažant, Z. P., "Numerical Determination of Long-Range Stress History from Strain History in Concrete," *Materials and Structures*, Paris, France, Vol. 5, No. 27, 1972, pp. 135–141.
3. Bažant, Z. P., and Najjar, L. J., "Comparison of Approximate Linear Methods for Concrete Creep," *Journal of the Structural Division*, ASCE, Vol. 99, No. ST9, Proc. Paper 10006, Sept., 1973, pp. 1851–1874.
4. Bažant, Z. P., "Theory of Creep and Shrinkage in Concrete Structures: A Précis of Recent Developments," *Mechanics Today*, Vol. 2, Pergamon Press, New York, N.Y., 1975, pp. 1–93.
5. Bažant, Z. P., and Osman, E., "Double Power Law for Basic Creep of Concrete," *Materials and Structures* (RILEM), Paris, France, Vol. 9, 1976, pp. 3–11.
6. Bažant, Z. P., and Bhat, P. D., "Prediction of Hysteresis of Reinforced Concrete Members," *Journal of the Structural Division*, ASCE, Vol. 103, No. ST1, Proc. Paper 12662, Jan., 1977, pp. 153–167.
7. Bažant, Z. P., and Panula, L., "Practical Prediction of Time-Dependent Deformations of Concrete," *Materials and Structures*, Paris, France, Parts I and II, Vol. 11, No. 68, 1978, pp. 307–328; Parts III and IV, Vol. 11, No. 69, 1978, pp. 415–434; Parts V and VI, Vol. 12, No. 72, 1979, pp. 169–183.
8. Bažant, Z. P., and Kim, S.-S., "Nonlinear Creep of Concrete—Adaptation and Flow," *Journal of the Engineering Mechanics Division*, ASCE, Vol. 105, No. EM3, Proc. Paper 14654, June, 1979, pp. 429–446.
9. Brettle, H. J., "Increase in Concrete Modulus of Elasticity due to Prestress and Its Effect on Beam Deflection," *Constructional Review*, Sydney, Australia, Vol. 31, No. 8, Aug., 1958, pp. 32–35.
10. Bridge, R. Q., "Composite Columns under Sustained Load," *Journal of the Structural Division*, ASCE, Vol. 105, No. ST3, Proc. Paper 14442, Mar., 1979, pp. 563–576.
11. "Building Code Requirements for Reinforced Concrete," *ACI Standard 318-77*, American Concrete Institute, Detroit, Mich., 1977.
12. Cook, R. D., *Concepts and Applications of Finite Element Analysis*, John Wiley and Sons, Inc., New York, N.Y., 1974.
13. Drysdale, R. G., and Huggins, M. W., "Sustained Biaxial Load on Slender Concrete Columns," *Journal of the Structural Division*, ASCE, Vol. 97, No. ST5, Proc. Paper 8103, May, 1971, pp. 1423–1443.
14. Fouré, B., "Le Flambement des Poteaux Compte Tenu du Fluage du Béton," *Annales de l'Institut Technique du Bâtiment et des Travaux Publics* (Théories et Méthodes de Calcul No. 214), Paris, France, No. 359, Mar., 1978, pp. 4–58.
15. Freudenthal, A. M., and Roll, F., "Creep and Creep Recovery of Concrete under High Compressive Stress," *American Concrete Institute Journal*, Vol. 54, 1958, pp. 1111–1142.
16. Gallagher, R. H., *Finite Element Analysis: Fundamentals*, Prentice-Hall, Inc., Englewood Cliffs, N.J., 1975.
17. Hellesland, J., and Green, R., "A Stress and Time-Dependent Strength Law for Concrete," *Cement and Concrete Research*, Vol. 2, 1972, pp. 261–275.
18. Hughes, B. P., and Ash, J. E., "Some Factors Influencing the Long-Term Strength of Concrete," *Materials and Structures* (RILEM), Paris, France, Vol. 3, No. 14, 1970, pp. 81–84.
19. Kempner, J., "Creep Bending and Buckling of Linearly Viscoelastic Columns," *Technical Note 3136*, U.S. National Advisory Committee for Aeronautics, Jan., 1954.
20. Kempner, J., "Creep Bending and Buckling of Nonlinearly Viscoelastic Columns," *Technical Note 3137*, U.S. National Advisory Committee for Aeronautics, Jan., 1954.
21. Kordina, K angzeitversuche an Stahlbetonstützen," *Deutscher Ausschuss für*

Stahlbeton, Heft 250, W. Ernst und Sohn, Berlin, Germany, 1975, pp. 1–36.
22. Leong, T. W., and Warner, R. F., "Creep and Shrinkage in Reinforced Concrete Beams," *Journal of the Structural Division*, ASCE, Vol. 96, No. ST3, Proc. Paper 7150, Mar., 1970, pp. 509–533.
23. Lin, T. H., *Theory of Inelastic Structures*, John Wiley and Sons, Inc., New York, N.Y., 1968.
24. Manuel, R. F., and McGregor, J. G., "Analysis of Prestressed Reinforced Concrete Columns under Sustained Load," *American Concrete Institute Journal*, Vol. 64, 1967, pp. 12–23.
25. Mauch, S., and Holley, M. J., "Creep Buckling of Reinforced Concrete Columns," *Journal of the Structural Division*, ASCE, Vol. 89, No. ST4, Proc. Paper 3610, Aug., 1963, pp. 451–481.
26. Mauch, S. P., "Effect of Creep and Shrinkage on the Capacity of Concrete Columns," Symposium on Reinforced Concrete Columns, *Special Publication SP-50*, American Concrete Institute, Detroit, Mich., 1966, pp. 299–324.
27. McClure, G. S., Jr., Gerstle, K. H., and Tulin, L. G., "Sustained and Cyclic Loading of Concrete Beams," *Journal of the Structural Division*, ASCE, Vol. 99, No. ST2, Proc. Paper 9564, Feb., 1973, pp. 243–257.
28. McHenry, D., "A New Aspect of Creep in Concrete and Its Application to Design," *Proceedings*, American Society for Testing and Materials, Vol. 43, 1943, pp. 1069–1086.
29. Mozer, J. D., Gerstle, K. H., and Tulin, L. G., "Time-Dependent Behavior of Concrete Beams," *Journal of the Structural Division*, ASCE, Vol. 96, No. ST3, Proc. Paper 7157, Mar., 1970, pp. 597–612.
30. Ross, A. D., "Creep of Concrete under Variable Stress," *American Concrete Institute Journal*, Vol. 54, 1958, pp. 739–758.
31. Rüsch, H., "Researches toward a General Flexural Theory for Structural Concrete," *American Concrete Institute Journal*, Vol. 57, 1960, pp. 1–28.
32. Sackman, J. L., and Nickell, R. E., "Creep of a Cracked Reinforced Beam," *Journal of the Structural Division*, ASCE, Vol. 94, No. ST1, Proc. Paper 5764, Jan., 1968, pp. 283–308.
33. Stöckl, S., "Tatversuche über den Einfluss von vorangegangegen Dauerlasten auf die Kurzzeitfestigkeit des Betons," *Deutscher Ausschuss für Stahlbeton*, Heft 196, W. Ernst und Sohn, Berlin, Germany, 1967, pp. 1–27.
34. Washa, G. W., and Fluck, P. G., "Effect of Sustained Loading on Compressive Strength and Modulus of Elasticity of Concrete," *American Concrete Institute Journal*, Vol. 48, May, 1950, pp. 693–700.
35. Washizu, K., *Variational Methods in Elasticity and Plasticity*, 2nd ed., Pergamon Press, New York, N.Y., 1975.
36. Wilhelm, W. J., and Zia, P., "Effect of Creep and Shrinkage on Prestressed Concrete Columns," *Journal of the Structural Division*, ASCE, Vol. 96, No. ST10, Proc. Paper 7614, Oct., 1970, pp. 2103–2123.
37. Wu, H., and Huggins, M. W., "Size and Sustained Load Effects in Concrete Columns," *Journal of the Structural Division*, ASCE, Vol. 103, No. ST3, Proc. Paper 12787, Mar., 1977, pp. 493–506.
38. Zienkiewicz, O. C., *The Finite Element Method in Engineering Science*, 2nd ed., McGraw-Hill Book Co., Inc., London, England, 1971.

ABSTRACT: This model accounts not only for the rapid increase of creep at high compressive stress (flow) but also for the decrease of creep observed for subsequent load increments after a long period of low sustained compressive stress (adaptation). A simply supported column is analyzed for typical load histories: sustained loading; short-time loading to failure; and sustained load followed by short-time loading to failure. Numerical results confirm that the flow nonlinearity makes the column fail in a finite time and the adaptation nonlinearity makes the response to the short-time load applied after a long period of a low sustained load stiffer. Also, there is a substantial difference in the column strength for the same load duration depending upon the loading history, especially the ratio of constant sustained load (dead load) and short-time load (live load) and their durations. This could be taken into account in setting the safety factors for columns subjected to dead and live loads of various ratios.

15811 NONLINEAR CREEP BUCKLING OF R.C. COLUMNS

KEY WORDS: **Buckling; Building codes; Columns (supports); Concrete (reinforced); Creep; Dead loads;** Design; Finite elements; **Live loads;** Loading; Numerical analysis; Shrinkage; Stability; Viscoelasticity

REFERENCE: Bazant, Zdenek P., and Tsubaki, Tatsuya, "Nonlinear Creep Buckling of Reinforced Concrete Columns," *Journal of the Structural Division*, ASCE, Vol. 106, No. ST11, **Proc. Paper 15811**, November, 1980, pp. 2235-2257